JOURNAL OF MATERIALS SCIENCE LETTERS 15 (1996) 1767–1769

Dielectric strength of fine grained barium titanate ceramics

T. TUNKASIRI, G. RUJIJANAGUL
Department of Physics, Faculty of Science, Chiang Mai University, Chiang Mai, Thailand 50200

The effects of particle and grain sizes on the properties of ferro-electric materials have been studied by many authors [1–5] and it has been confirmed that the physical properties have optimum values depending on these parameters (the particle and grain size). For example, the c/a ratio of the unit cell of $BaTiO_3$, measured for powders, was found to have a maximum value when the particle size was approximately 0.4 μm [5]. Also it has been shown [1, 2] that the relative permittivity, ε_r, depended on the grain size of the ceramics in the range 0.7–53 μm, and Yamashita *et al.* [6], found that the dielectric strength of the $BaTiO_3$ ceramics increased with decreasing grain size. In the cases of [6, 7], the experimental data related to ceramics having grain sizes larger than 25 μm. In contrast, this study is concerned with the dielectric strength of barium titanate ceramics having grain sizes less than 25 μm. A chemical route was used to prepare barium titanate starting powder having a particle size less than 0.1 μm and the grain size of the ceramic was varied by varying the sintering temperature.

Barium titanyl oxalate tetrahydrate [$BaTiO(C_2O_4)_2.4H_2O$] powder was prepared following [8, 9]. The powder was filtered, dried and heated at 1000 °C for 1 h to yield a homogeneous $BaTiO_3$ powder of small (<1 μm) particle size. The powder was processed into disc shapes of about 1.2 mm thick and 25 mm diameter, using polyvinyl alcohol (2 wt %) as a binder. To vary the grain size, the discs were sintered at 1320, 1330, 1350, 1380 and 1400 °C; the peak temperatures being held for 2 h in each case. Five samples were prepared for each sintering temperature. X-ray diffractometry was employed to identify the phases, and the densities were determined. The discs were ground to a standard thickness of 1 mm and electrodes applied to both faces using conducting silver paste. To determine electric breakdown strength, each sample was clamped between a pair of hemispherical brass electrodes and placed in a cell built following the design of Owate and Freer [10]. The cell was immersed in transformer oil, heated to 60 °C, pumped by a rotary pump to remove air bubbles and then cooled to room temperature before testing. A direct current (d.c.) voltage was applied from a commercial power supply (Hipotronics Inc. model HD 100). The rate of voltage increase was 30 $V\,s^{-1}$. After the breakdown test, the samples were ground, polished and thermally etched. The microstructure was observed using scanning electron microscopy (SEM), and the grain sizes were determined by the line intercept method [11]. The total porosity values were calculated by comparison of the measured densities with a single crystal value.

Fig. 1 shows scanning electron micrographs for the extremes of the sintering conditions. As expected, the grain size is smaller at the lower extreme temperature; also, the grain size distributions at the lower sintering temperatures are more uniform than those for the samples sintered at higher temperatures. The grain sizes lie in the range 3.5–25 μm and the corresponding electric strengths in the range 8.5–2.5 $kV\,mm^{-1}$, as shown in Fig. 2. Each quoted electric strength value is the mean of measurements made on five different specimens. The total porosity values are listed in Table I.

X-ray diffraction (XRD) confirmed the specimens to be $BaTiO_3$ [12]. The (2 0 0) and (0 0 2) reflections are shown in Fig. 3, indicating the tetragonal phase; however, the structure tends towards cubic for lower sintering temperatures. It should be noted that only

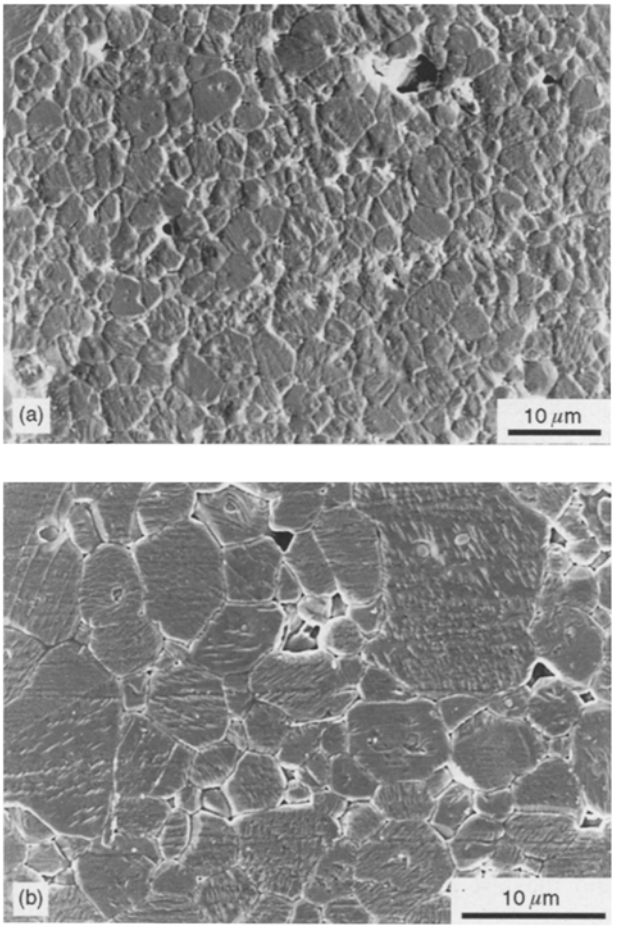

Figure 1 Scanning electron micrographs of $BaTiO_3$ ceramics sintered at (a) 1320 °C for 2 h, and (b) 1400 °C for 2 h.

0261-8028

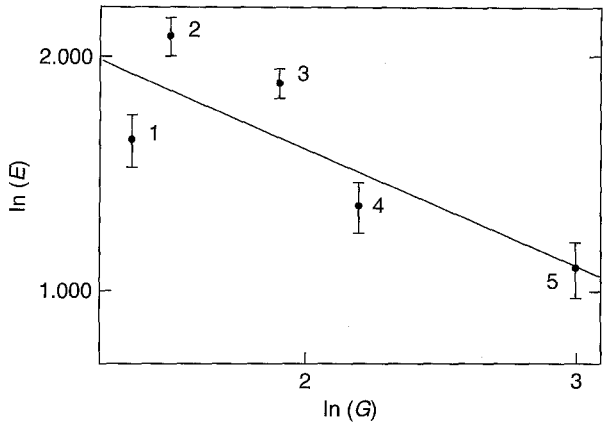

Figure 2 Grain size dependence on dielectric strength. Numbers indicate sintering temperatures: (1) 1320 °C, (2) 1330 °C, (3) 1350 °C, (4) 1380 °C, (5) 1400 °C.

TABLE I Density and porosity of $BaTiO_3$ ceramics for different sintering temperatures

Sintering temperature (°C)	*c/a*	Density ($Mg\,m^{-3}$)	Total porosity (%)[a]
1320	1.0030	5.85	2.82
1330	1.0096	5.74	4.65
1350	1.0126	5.72	4.98
1380	1.0094	5.73	4.82
1400	1.0103	5.74	4.65

[a]Calculated assuming a crystal density of $6.02\,Mg\,m^{-3}$.

the 'cubic' phase of $BaTiO_3$ was found by Schomann [7] who prepared his specimens by isostatic hot-pressing at 1250 °C. The dielectric strengths measured by Schomann were higher than those measured in this study: this may be related to differences in preparation methods in the two studies.

Fig. 4 shows the breakdown track and a crater; similar craters were formed on both faces of the specimens. Fig. 5 shows the molten material that surrounded the craters. Similar breakdown features have been observed by Owate and Freer [10] in their studies on alumina ceramics. The crater structure and the edge-marking along the breakdown channel appear to be formed by local melting accompanying the breakdown process and subsequent recrystallization.

The data in Fig. 2 fit the relation, $E\alpha G^{-a}$, where E, G and a are, respectively, the breakdown field-strength, grain size and a constant; the value of a is approximated 0.5. Similar results were obtained by Beauchamp [13] for the electrical strength of MgO ceramics, and by Pohanka *et al.* [14] for the mechanical fracture strength of $BaTiO_3$ ceramics.

In the case of mechanical failure, a pore size related to the grain size acts as the critical defect. When the enhanced stress in the immediate vicinity of the stress-raising pore in the material reaches a critical value crack initiation and propagation occur and the test piece fails. Similar arguments can be advanced to explain electrical breakdown; in that the breakdown starts at the grain boundaries, probably at pores on the grain boundaries or surface flaws in the samples, as pointed out in [13, 15].

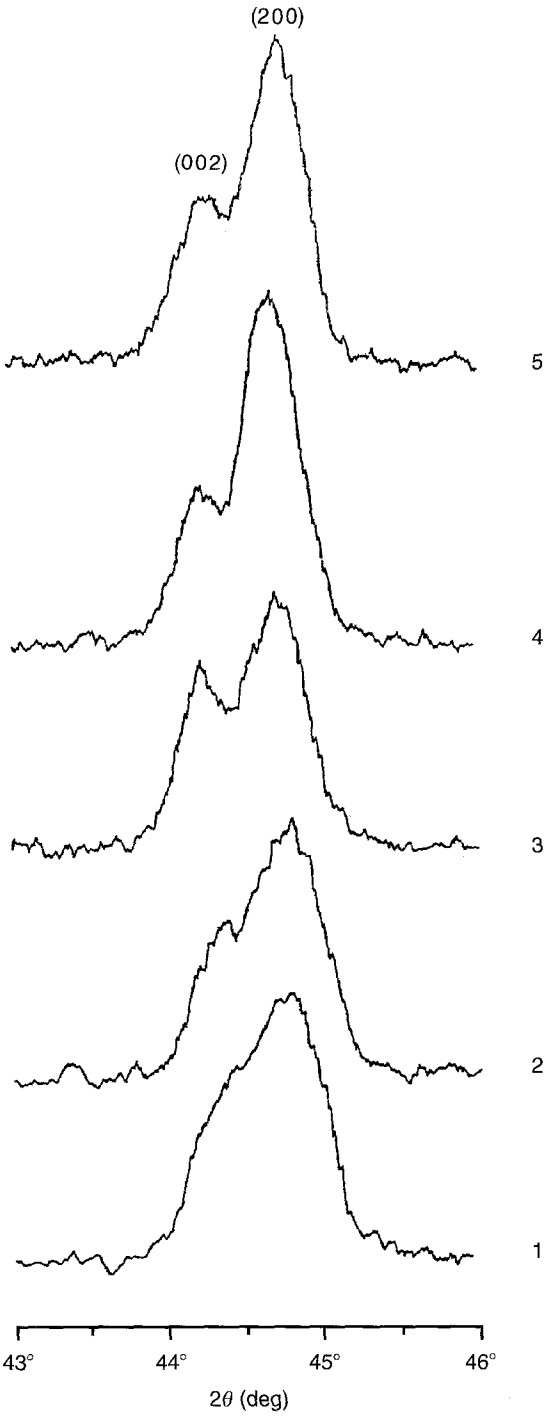

Figure 3 Changes in the (2 0 0) and (0 0 2) reflections with sintering temperature (sintering temperatures of samples 1–5 are given in Fig. 2).

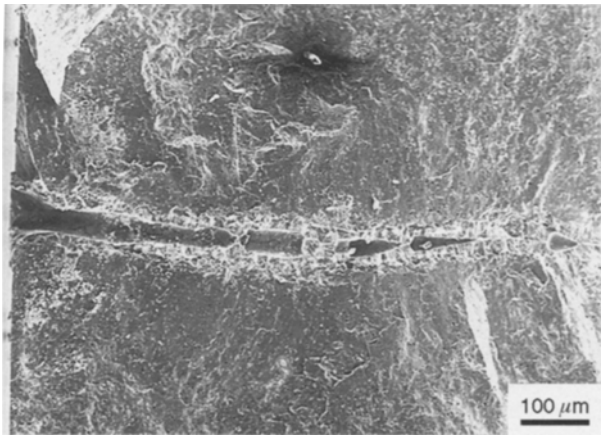

Figure 4 Conduction channel after breakdown.

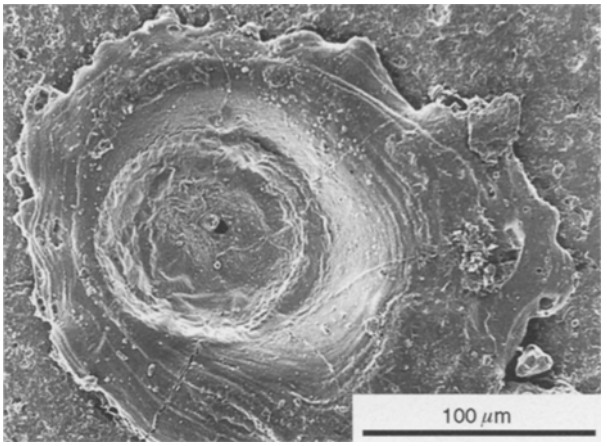

Figure 5 Crater surface after breakdown.

In conclusion, there is a tendency for $BaTiO_3$ ceramics to assume a cubic crystal structure as the sintering temperature is reduced. Smaller grain size inhibits 90° domain formation and hence tends to hold the structure in the high temperature cubic phase [2]. This study shows the same tendency to the cubic phase in barium titanate ceramics derived from a chemically prepared powder, as the sintering temperature decreases in the range 1400–1320 °C. The form of the breakdown features is similar to that observed by Owate and Freer [10] and suggests that local melting accompanies the breakdown. The relationship between breakdown strength and grain size is of the same form as observed for the mechanical strength of ceramics, and confirms that a clear parallel can be drawn between the two (insofar as microstructure defects, of a size related to the grain size, are the critical defects from which failure is initiated).

Acknowledgements

The authors would like to express their sincere thanks to the National Metal and Materials Technology Centre of Thailand for funding this project.

References

1. K. KINOSHITA and A. YAMAJI, *J. Appl. Phys.* **47** (1976) 371.
2. G. ARLT, D. HÉNNINGS and G. DEWITH, *ibid.* **58** (1985) 1619.
3. H. C. GRAHAM and N. M. TALLAN, *J. Amer. Ceram. Soc.* **54** (1971) 548.
4. K. ISHIKAWA, K. YOSHIKAWA and N. OKADA, *Phys. Rev. B* **37** (1988) 5852.
5. K. UCHINO, E. SADANAGA and T. HIROSE, *J. Amer. Ceram. Soc.* **72** (1989) 1555.
6. K. YAMASHITA, K. KOUMOTO, M. TAKATA and H. YANAGIDA, *Jpn. J. Appl. Phys.* **19** (1980) 867.
7. K. D. SCHOMANN, *J. Appl. Phys.* **6** (1975) 89.
8. F. S. YEN, C. T. CHANG and Y. H. CHANG, *J. Amer. Ceram. Soc.* **73** (1990) 3422.
9. T. TUNKASIRI and G. RUJIJANAGUL, *J. Mater. Sci. Lett.* **13** (1994) 165.
10. I. O. OWATE and R. FREER, *J. Appl. Phys.* **72** (1992) 2418.
11. 'Annual Book of ASTM Standards, Designation E: 112-82' (Easton, MD, 1992).
12. 'Powder Diffraction File', Joint Committee on Powder Diffraction Standards, (International Center for Diffraction Data, Swarthmore, PA, 1987) Card No. 5-626.
13. E. K. BEAUCHAMP, *J. Amer. Ceram. Soc.* **54** (1971) 484.
14. R. C. POHANKA, R. W. RICE and B. E. WALKER JR, *ibid.* **59** (1976) 71.
15. A. KISHIMOTO, K. KOUMOTO and H. YANAGIDA, *J. Mater. Sci.* **24** (1989) 698.

Received 26 February
and accepted 17 June 1996